

# Elastic/Plastic Indentation Damage in Ceramics: The Lateral Crack System

D. B. MARSHALL,\* B. R. LAWN,\*\* and A. G. EVANS\*

Department of Materials Science and Engineering, University of California, Berkeley, California 94720

The mechanics of lateral crack propagation in a sharp-indenter contact field are described. The driving force for fracture has its origin in the residual component of the elastic/plastic field, which becomes dominant as the indenter is unloaded. Expressions for equilibrium crack evolution are derived, with due allowance for the close proximity of crack plane and specimen free surface. As with the median/radial crack system considered in an earlier paper, the ratio hardness-to-modulus complements toughness in the fracture relations. The basic predictions of the theory are examined in terms of experimental measurements of lateral crack dimensions in materials with a wide range of mechanical properties. The prospects of predicting the extent of lateral fracture in other ceramics, and thence of establishing a base for analyzing such important practical properties as surface erosion, are discussed.

## I. Introduction

THE fracture associated with elastic/plastic contact on brittle surfaces is of two basic types, "median/radial" and "lateral." An earlier study dealt with the first of these types.<sup>1</sup> Emphasis was placed on the role of deformation processes in driving the cracks: hardness  $H$  and stiffness  $E$ , in addition to toughness  $K_c$ , accordingly entered as controlling material parameters. All basic features of the median/radial crack evolution during the indentation cycle were found to be predictable by linear fracture mechanics analysis.

The intent of the present paper is to develop a similar analysis for the lateral crack system. Lateral cracks are observed to initiate near the base of the plastic deformation zone below the contact, and to spread out laterally on a plane closely parallel to the specimen surface.<sup>2-5</sup> In a severe contact event these cracks can run to the surface to cause material removal. The first systematic observations of sharp-contact fracture, in glass,<sup>2</sup> showed that the lateral extension occurs during indenter unloading, in much the same way as the surface radials.<sup>1</sup> Subsequent work on other ceramics<sup>5</sup> showed similar trends. Residual stresses were thereby identified as the primary driving force for lateral cracking. For want of a suitable theoretical model for handling this type of stress field, the lateral system has not hitherto been subjected to first-principles analysis—rather, semiempirical formula fits have been adopted for specific applications.<sup>5</sup> In view of the key role played by lateral fracture in the erosion<sup>6,7</sup> and wear<sup>8,9</sup> of brittle surfaces, an attempt at a fundamental study would appear to be opportune.

The treatment presented here follows that of the median/radial analysis.<sup>1</sup> Thus, the elastic/plastic contact field is considered in terms of superposed elastic and residual crack driving forces. As with the median/radial system, the crack geometry is taken to be pennylike, but with the complication of an adjacent, parallel free surface. Again, only the crack propagation stage is considered.

## II. Lateral Fracture Model

### (1) Basic Description

Consider the idealized lateral crack system in Fig. 1. The contact at load  $P$  leads to a crack of characteristic radius  $c$ , at depth  $h$  below the surface. The plastic zone supports the indenter, included angle  $2\psi$  (not shown), over the characteristic radius  $a$ , and extends outward to a radius  $b$ . At this point it is unnecessary to recognize the existence of the median/radial system in the construction of the model, even though this system precedes the expansion of the lateral crack in the contact cycle—crack interaction effects may be introduced more conveniently as a geometrical perturbation later in the analysis (Section II(2)). A similar statement may be made about the coexistence of more than one lateral crack (as commonly observed in more severe contact events<sup>6</sup>)—the model of Fig. 1 represents the growth of a primary lateral crack.

With the emphasis on crack propagation, details in the complex near field of the elastic/plastic contact do not need to be specified. The threshold conditions for lateral fracture are thereby excluded from the present analysis. It is nevertheless important to appreciate that a residual tensile stress develops at the nucleation center near the base of the deformation zone, so that a residual driving force  $P_r$  acts on the crack as the indenter is withdrawn (Fig. 1). In the absence of reversed plasticity within the central zone,<sup>1</sup>  $P_r$  reaches its maximum at full contact loading, and persists at this value on removal of the indenter. Thus, consistent with the procedure adopted in Ref. 1, the net mouth-opening force for the system may be expressed as the difference between an irreversible residual (opening) component and a reversible elastic (closing) component. Experimental observations indicate that lateral cracks initiate as the diminishing applied load approaches zero (Section III). Therefore the following analysis will be concerned only with the final unloaded configuration.

### (2) Stress Intensity Factor

In accordance with the indentation fracture mechanics approach,<sup>3</sup> a stress intensity factor is sought for the configuration of Fig. 1 in terms of contact load and crack size. It is not appropriate to use the standard formula for embedded pennylike cracks,<sup>1</sup> because of the presence of the specimen free surface. The importance of the free-surface influence may be inferred from the considerable uplift that is evident about the impression zone, as in Fig. 2;

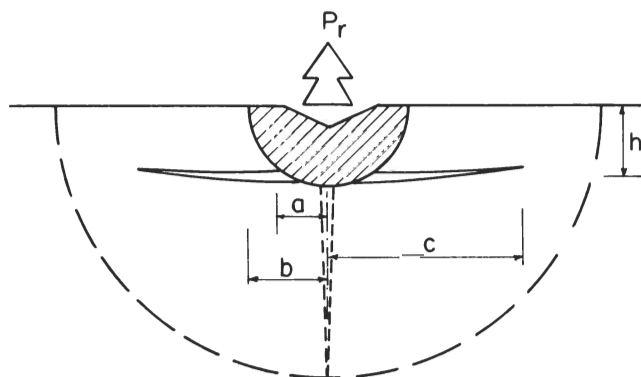


Fig. 1. Lateral crack system. Residual force,  $P_r$ , exerted by radially expanded plastic zone determines crack-driving force. Broken lines indicate median/radial crack system.

Presented at the 83rd Annual Meeting, The American Ceramic Society, Washington, DC, May 6, 1981 (Basic Science Division No. 156-B-81). Received February 15, 1982; revised copy received May 20, 1982; approved May 26, 1982.

Supported by the U. S. Office of Naval Research under Grant No. N00014-81-K-0362 and by the Australian Research Grants Committee.

\*Member, the American Ceramic Society.

\*\*At the time this work was done, B. R. Lawn was on study leave from the University of New South Wales, New South Wales, Australia. He is now with the Fracture and Deformation Division, National Bureau of Standards, Washington, DC 20234.

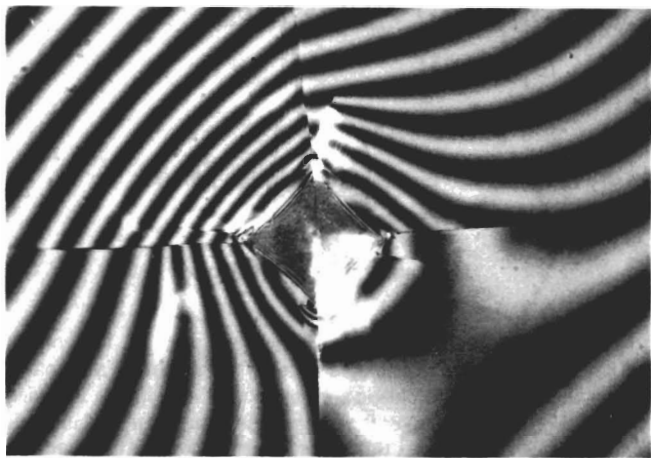


Fig. 2. Vickers indentation ( $P=50$  N) in soda-lime glass; interference fringe micrograph, sodium light. Fringe distortion indicates surface uplift of material above lateral crack plane. Note distortion contained within bounds of radial crack traces (width of micrograph =  $625 \mu\text{m}$ ).

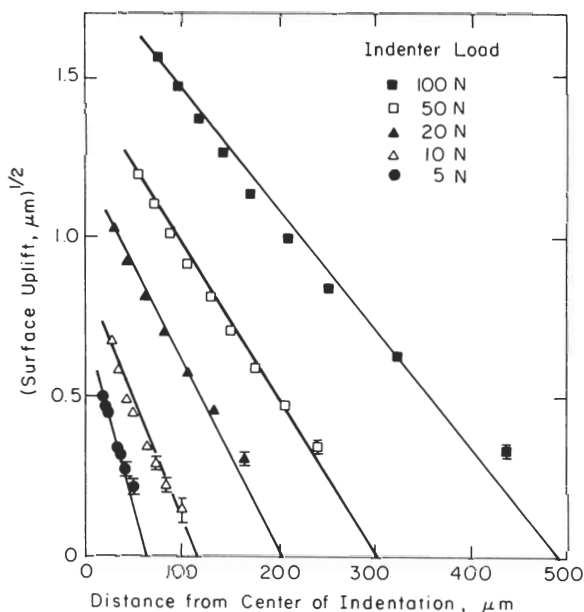


Fig. 3. Profiles of surfaces adjacent Vickers indentations in soda-lime glass. Measurements from optical interference micrographs; where error bars are not shown, measurement errors are smaller than data points.

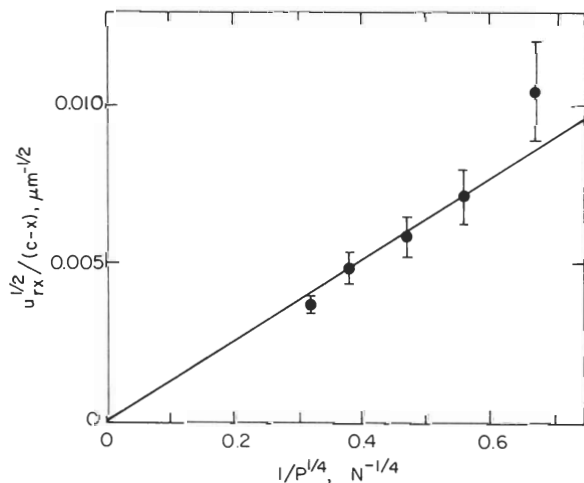


Fig. 4. Plot of measured (negative) gradients from Fig. 3 as a function of contact load parameter.

the disk of material above the crack plane is relatively free of bulk constraint, and must accordingly be expected to accommodate the greater proportion of the system's mechanical energy. No such uplift is observed around crack-free indentations. Close analogy between this configuration and that treated by Obreimoff<sup>10</sup> (see, for example, Ch. 1 of Ref. 11) in his classical study of the cleavage of mica suggests that the lateral crack may be usefully modeled in terms of simple plate theory.<sup>12</sup> Conveniently, such an approach would be expected to be most accurate for  $c \gg h$ , i.e. in the requisite region of full crack propagation.

The analysis takes the material above the crack plane in Fig. 1 to be loaded elastically along its axis with force  $P_r$  and to be effectively "built-in" at radial distance  $c$ . The material below is much less compliant, and may therefore be treated as a rigid substrate. Then if  $u_r$  is the net load-point displacement at the disk center, a linear compliance relation of the form  $u_r = \lambda P_r$  may be written for the crack system. A general displacement solution for a plate of Young's modulus  $E$  and Poisson's ratio  $\nu$  loaded in this way is

$$\lambda = Ac^2/Eh^3 \quad (1)$$

where  $A$  is a dimensionless, geometrical constant. Detailed discussion of Eq. (1) is given in Appendix A, where two specific lateral/radial configurations are considered: (i) laterals  $\gg$  radials (full-plate approximation), giving  $A = 3(1-\nu^2)/4\pi$ ; (ii) laterals  $<$  radials (quarter-plate approximation), giving  $A = 3/4$ . The effect of preexistent radial cracks on lateral fracture mechanics is therefore accommodated by a simple adjustment in system compliance.

With the compliance thus determined, the crack extension force,  $G$ , follows directly from the standard formula (see Ch. 3 of Ref. 11)

$$G = (P_r^2/2)d\lambda/dC \quad (2)$$

where  $C = \pi c^2$  is the crack area. Inserting Eq. (1) into Eq. (2), and making use of the equivalence relation  $G = K^2(1-\nu^2)/E$  for plane strain fracture, the stress intensity factor is calculated as

$$K = [A/2\pi(1-\nu^2)]^{1/2} P_r/h^{3/2} \quad (3)$$

This result warrants special comment here. Noting that  $[A/2\pi(1-\nu^2)]^{1/2}$  is a constant, the stress intensity factor is of the same form as that used for median/radial cracks,<sup>1</sup> but with the dimension  $h$  replacing  $c$ . The absence of any explicit term in crack length in Eq. (3) would appear to be inconsistent with the experimental observation that lateral cracks propagate in a highly stable manner. However, because of the relatively high compliance of the lateral system, it may be expected that the residual force  $P_r$  will relax significantly as propagation proceeds, thus making  $K$  a diminishing function of  $c$ . Specification of  $P_r(c)$  accordingly becomes central to any fracture mechanics determination.

### (3) Compliance Relation for Central Deformation Zone

It is now necessary to consider the mechanical characteristics of the central deformation zone. Recalling the sequence of operations used to evaluate the residual stress term in Ref. 1 (Section II(2A), Appendix A), it is expedient to adopt the analog of a precompressed linear spring. Then the residual force may be expressed as

$$P_r/P_{r0} = 1 - u_r/u_{r0} \quad (0 \leq u_r \leq u_{r0}) \quad (4)$$

where  $P_{r0}$  is the force exerted by the spring element in the fully compressed state (i.e. at  $u_r = 0$ ) and  $u_{r0}$  is the displacement in the fully relaxed state ( $P_r = 0$ ). Since displacement is a much less accessible variable than load in contact testing, it is useful to use the linear compliance relation  $u_r = \lambda P_r$  in conjunction with Eq. (1) to eliminate  $u_r$  from Eq. (4):

$$P_r = P_{r0}/(1 + AP_{r0}c^2/Eu_{r0}h^3) \quad (5)$$

The parameters  $P_{r0}$ ,  $u_{r0}$ , and  $h$  provide the means for incorporating the elastic/plastic properties of the material into the formulation. To determine these parameters, expressions are first written for the characteristic dimensions of the plastic zone (Ref. 1,